

Article:

Reusable Ionogel-based Photo-actuators in a Lab-on-a-disc

Janire Saez, Tom Glennon, Monika Czugala, Alexandru Tudor, Jens Ducreé, Dermot Diamond, Larisa Florea, Fernando Benito-Lopez

Sensors and Actuators B: Chemical 257 : 963–970 (2018)

This work is made available online in accordance with publisher policies. To see the final version of this work please visit the publisher's website. Access to the published online version may require a subscription.

Link to publisher's version:

<http://doi.org/10.1016/j.snb.2017.11.016>

Copyright statement: © 2017 Elsevier Ltd. Full-text reproduced in accordance with the publisher's self-archiving policy.

This manuscript version is made available under the CC-BY-NC-ND 4.0 license <http://creativecommons.org/licenses/by-nc-nd/4.0>



REUSABLE IONOGE-BASED PHOTO-ACTUATOR VALVES IN A LAB-ON-A-DISC PLATFORM

Janire Saez,¹ Tom Glennon,^{2,3} Monika Czugała,² Alexandru Tudor,² Jens Ducreé,³ Dermot Diamond,² Larisa Florea,² Fernando Benito-Lopez^{1,*}

¹Analytical Microsystems & Materials for Lab-on-a-Chip (AMMa-LOAC) Group, Microfluidics Cluster UPV/EHU, Analytical Chemistry Department, University of the Basque Country UPV/EHU, Vitoria-Gasteiz, Spain

²Insight Centre for Data Analytics, National Centre for Sensor Research, Dublin City University, Dublin 9, Ireland

³School of Physical Sciences, National Centre for Sensor Research, Dublin City University, Dublin 9, Ireland

Abstract

This paper describes the design, fabrication and performance of a reusable ionogel-based photo-actuator, *in-situ* photopolymerised into a lab-on-a-disc microfluidic device, for flow control. The ionogel provides an effective barrier to liquids during storage of reagents and spinning of the disc. A simple LED (white light) triggers actuation of the ionogel for selective and precise channel opening at a desired location and time. The mechanism of actuation is reversible, and regeneration of the actuator is possible with an acid chloride solution. In order to achieve regeneration, the Lab-on-a-Disc device was designed with a microchannel connected perpendicularly to the bottom of the ionogel actuator (regeneration channel). This configuration allows the acid solution to reach the actuator, independently from the main channel, which initiates ionogel swelling and main channel closure, and thereby enables reusability of the whole device.

1 Introduction

Centrifugal microfluidics, commonly known as 'Lab-on-a-Disc' (LoaD) has many advantages over other microfluidic approaches. These include (i) minimal amount of fluidic manipulation components since liquids are moved by centrifugal forces, (ii) the absence of bubbles after

efficient spinning, (iii) minimal dead volume and (iv) the possibility of performing complex assays with no external energy input, facilitating their use in resource-limited environments.^{1,2}

The use of LoaD technology enables the fabrication of simple, stand-alone instrumentation with a simple spindle motor, without the need of complicated and expensive peripherals such as tubing connections and pumps. Moreover, reagents can be pre-stored and used on demand.³

Among all the possible microfluidic operations that can be implemented in a disc, valving is one of the most important, since it allows flow manipulation and control in the microchannel. In LoaDs,³⁻⁸ closed passive valves are the most extensively investigated since they are easily actuated by controlling the spinning speed of the disc. The inherent geometry, position and physical properties of these valves in the microfluidic channel governs their open or closed state. In general, passive valves are easily fabricated, following conventional microfabrication methods; however, to accurately control their actuation remains difficult, especially when attempting to control individual valves in devices that have multiple valves. Moreover, any microfabrication inaccuracy adversely affects the flow during spinning and thereby the performance of the valve.

In order to achieve simple and robust flow control, many kinds of active valves have recently been investigated.¹ These include valves based on wax,^{9, 10} dissolvable films¹¹⁻¹³ and photoswitchable polymer actuators. Active valves are triggered by external sources and can be switched between an open and a close state during the spinning process.¹ However, these valves are difficult to implement into a centrifugal microfluidic device, since they are often manually integrated, resulting in high fabrication costs and actuation inaccuracy.

Stimuli responsive materials, can present switchable chemical properties, mechanical strength, tuneable permeability and mouldable surface characteristics among others. Typically, these are controlled by applying an external stimulus (light, temperature, chemical, magnetic field, etc.). They are porous macromolecular structures formed by crosslinked monomers that absorb water to generate a gel-like network known as a hydrogel. The stimuli responsiveness of these materials is based on the existence of two metastable energy states associated with two structural forms that possess distinctly different energy minima.¹⁴ It is described that the mechanisms of switching of these materials is achieved when a relative large number of molecules populating these energy states can be externally perturbed with a stimulus (*e.g.* light) and so switched from one dominant state to the other. It is clear that the functional groups

present in the gel network are the responsible of the type of actuation of the gel (*eg.* magnetic, thermal, optical, mechanical, or chemical).

Stimuli responsive gels such as the poly(*N*-isopropylacrylamide), p(NIPAAm), have been deeply investigated as thermoactuators.¹⁵⁻¹⁸ The swelling degree of p(NIPAAm) is very high at low temperatures due to high water uptake, and this state changes abruptly upon crossing its lower critical solution temperature (LCST), leading to contraction to a compact globular form due to release of water.¹⁹ A similar behaviour can be achieved using light as a non-contact and non-invasive stimulus. Light irradiation represents one of the most attractive actuation mechanisms which is exhibited when p(NIPAAm) gels are functionalised with spirobenzopyran moieties (SP).²⁰ Spirobenzopyrans can be switched upon light irradiation between two states, which are thermodynamically stable.²¹ These hybrid materials, referred as p(SPNIIPAAm) from now on, have two stimuli responsive functions: first, thermoresponsive p(NIPAAm) gels are swollen below the LCST and secondly, the photoresponsive SP molecule, when open to the charged merocyanine (MC-H⁺) isomer under UV-irradiation, is able to convert to the uncharged SP isomer under light irradiation. The switching mechanism, from MC-H⁺ to SP isomer, is reversible and triggers conformational rearrangements in the bulk p(NIPAAm) gel, changing it from a more hydrophilic to a hydrophobic nature, which in turn induces water loss and contraction of the gel.²²

Traditionally, organic solvents have been employed for the synthesis of p(SPNIIPAAm) gels. However, more recently, the incorporation of ionic liquids (ILs) as solvents within the gel polymer matrix is generating a lot of attention, as the new class of materials, known as ionogels, can exhibit very attractive characteristics, as they can retain the physical properties of both the polymer gel and the physically entrapped IL. Recent reviews have examined the interactions between the entrapped IL with the polymer network of the ionogel, as well as the use of ionogels as sensors and actuators.²³ ILs generally offer excellent chemical and thermal stability, high ionic conductivity, low vapour pressure, and tuneable hydrophobicity and hydrophilicity, depending on the particular cation-anion combination. Recently, ionogels were reported to exhibit improved water uptake/release behaviours and better mechanical and viscoelastic properties compared to their equivalent hydrogels.²⁴ Our group, successfully developed photo-actuators based on ILs incorporated within the p(SPNIIPAAm) gel. It was demonstrated that by using different ILs within the polymer matrix, the kinetics of the actuation could be controlled through IL mediation (rate of protonation/deprotonation), and through the movement of counter ions and solvent (water) in the ionogel matrix. As a consequence, ionogels containing different ILs

were found to respond at different times when exposed to a common light source in microfluidic devices.²⁵

Therefore, photo-switchable actuators are able to achieve non-contact, spatial independence and parallel fluid manipulation together with low cost and easy implementation, which are requirements for the improvement of functionalities such as valving in LoAD microfluidic devices. In conventional microfluidic devices, these actuators have been investigated previously. For example, Coleman *et al.*²⁶ developed a photo-valve that can be operated in microfluidic devices as a flow controller. Czugała *et al.*²⁷ developed a photo-switchable actuator that is capable of storage reagents when in the closed state. After actuation with white light it opens, allowing the reagent to flow to the main channel and react with the analyte of interest. However, to our knowledge, this type of valving mechanism has so far not been investigated in centrifugal platforms.

Herein we describe for the first time, the design, fabrication and performance of a reusable ionogel-based actuator, *in-situ* photopolymerised into a LoAD device to provide flow control functions. The ionogel provides a barrier to liquids during storage, and spinning of the disc up to 600 rpm. A white light LED, as source of irradiation, allows the selective opening, of the ionogel photovalve at a desired time. The regeneration of the actuator, i.e., closing, is possible with an acid chloride solution which contacts the valve via a microchannel connected to the bottom of the ionogel actuator, fabricated perpendicularly to the main channel to prevent ingress by the acid into the main fluidic channel.

2 Experimental

2.1 Materials and equipment

For the synthesis of the ionogels *N*-isopropylacrylamide, (*N,N'*-methylene-bis(acrylamide) (MBIS), the photo-initiator 2,2-dimethoxy-2-phenylacetophenone (DMPA) and the ionic liquid trihexyltetradecylphosphonium dicyanamide [P_{6,6,6,14}][dca], were purchased in Sigma Aldrich (St Louis, MO, USA). 1',3',3'-trimethyl-6-acrylate(2H-1-benzopyran,2'-indoline) was synthesised by us following the previously reported protocol from reference²⁸. 1 N HCl was purchased to Merck Millipore (Darmstadt, Germany).

The purification of the IL was carried out following the protocol published by us before, in short, 10 mL of IL were dissolved in 30 mL of acetone, then the solution was processed with activated

charcoal (Darco-G60, Aldrich®) at 40 °C overnight. Carbon was removed by filtration through alumina (acidic, Brockmann I, Aldrich®) and the solvent removed under vacuum at 60 °C for 24 h at 0.1 Torr.²⁹

The UV light source used for photo-polymerisation was a BONDwand UV-365 nm obtained from Electrolyte Corporation, USA.

The microfluidic devices were fabricated with a laser ablation system Epilog Zing 16 (Golden, USA). 1 mm thickness poly(methyl) methacrylate (PMMA) slides were purchased from Goodfellow, UK. ArCare® pressure sensitive adhesive (PSA) of 86 µm double side roll was generously provided by Adhesive Research (Limerick, Ireland) and cut using Graphtec CE5000-40 Craft Robo Pro (Tokyo, Japan). A thermal laminator roller ChemInstruments HL-101 (Fairfield, OH, USA) was used for PMMA and PSA layers bonding.

A homemade centrifugal instrument that incorporates a LED was used for studying the performance of the photo-actuators, (Figure SI1). A Dolan-Jenner LMI-6000 fiber optic illuminator (Edmund Optics, York, UK) was used for the actuation of the ionogels. For the visual monitoring of the liquid flow, red food dye (McCormick, Sabadell, Spain) was used.

Pictures were taken with Aigo Nexus GE5 digital camera and analysed using its software. 3D microscope pictures were taken by using a VHX-2000 3D Keyence 3D microscope and analysed using the 3D microscope's software.

2.2 p(SPNIpAAm) preparation and integration as actuator into the Lab-on-a-disc

The ionogel actuator (Figure 1A) was synthesised using an adapted version of the protocols described by Czugala *et al.*²⁹ and Saez *et al.*³⁰ Briefly, NIPAAm, MBIS and 1', 3', 3'-trimethyl-6-acrylate(2H-1-benzopyran-2,2'-indoline), 85.00 mg, 6.10 mg and 4.12 mg, respectively with the photo-initiator DMPA (2.68 mg) were dissolved in 285.95 mg of [P_{6,6,6,14}][dca]. The solution (3 µL) was photopolymerised in the actuator disc reservoir, filling the entire volume of the reservoir, through a mask using a UV-365 nm LED placed 8 cm far from the solution (UV intensity 10 mW cm⁻²) for 25 min. Upon completion of the polymerisation, the resulting ionogel actuators were rinsed with deionised water to remove any un-polymerised monomer and excess of ionic liquid. The ionogel actuators were dried at room temperature for 24 h. After assembly of the different layers of the Load platform, 10⁻³ M HCl aqueous solution was used to initially swell the valve actuators using the perpendicular channel, Figure 1B. The actuators were exposed to the

acidic solution for 2 h at room temperature to ensure the valve was swollen and the main channel closed. Furthermore, the ionogel actuator continuously blocked the perpendicular side channel, preventing fluidic transfer between the main channel and the perpendicular channel. After 2 h, the ionogel was irradiated with white light, which caused contraction of the gel, releasing H^+ and water molecules thus, opening the main channel to fluid movement (but maintaining the closed status of the perpendicular channel).

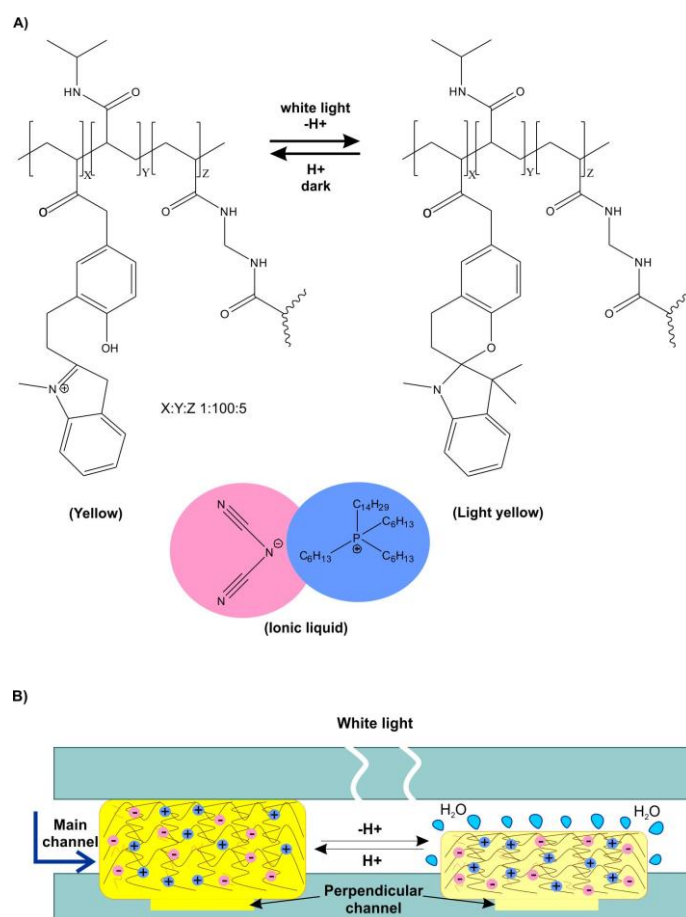


Figure 1: (A-top) Chemical structure of the crosslinked p(NIPAAm) gel functionalised with the SP, protonated (left) and deprotonated (right), and (A-bottom) chemical structure of the trihexyltetradecylphosphonium dicyanoamide ionic liquid; both components form the photoresponsive ionogel. (B) Schematic illustration of the reversible swollen (channel closed)/contracted (channel open) polymer network due to movement of protons (H^+) and water from the ionogel (not to scale).²⁷

2.3 Device fabrication and assembly

The device was created in a disc format, consisting of several PMMA and PSA layers aligned manually and bonded together in a laminator under controlled temperature. PMMA sheets were cut using a CO₂ laser while PSA sheets were cut by using xurography,³¹ both of which are rapid prototyping techniques. Figure 2 shows the structure of the LoAD device in terms of the following layers:

- 1) Bottom PMMA layer that seals the disc and contains the perpendicular channel and the reservoir in which the actuator is placed.
- 2) Lower PSA layer containing the channels (500 μm width) that connect the chambers (sample loading, actuation and bottom chamber) and bonds the bottom and middle PMMA layers.
- 3) Middle PMMA layer, containing all chambers (including a chamber for actuator visualisation).
- 4) Upper PSA layer that allows visual observation of the channels in the layers below and bonds top and middle PMMA layers.
- 5) A PMMA top layer, which contains the vents and loading holes.

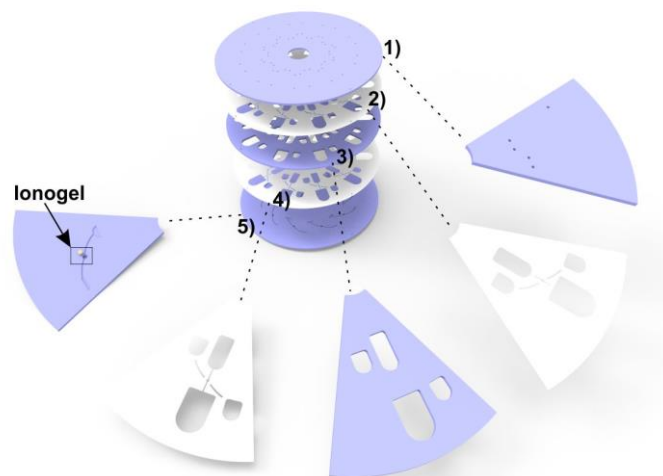


Figure 2: Assembly of the multi-layer LoAD device. 1) Lower PMMA layer seals the disc and contains the perpendicular channel and the reservoir in which the actuator is photopolymerised. 2) PSA layer containing the channels. 3) PMMA layer containing the chambers. 4) PSA layer seals layers 5 and 3 and ensures channel visualisation. 5) PMMA layer containing the vents and loading holes.

2.4 Characterisation of the actuator inside the LoAD

Studies of the swelling and shrinking kinetics of the actuator in the LoAD were carried out device as follows. A cross-section of the actuator and reservoir were cut with a CO₂ laser and pictures taken of the swelling with deionised water and shrinking by exposure to a white light LED placed at 1 cm from the actuator for a period of 25 minutes . The pictures were analysed via the Aigo Nexus GE5 digital microscope camera software and the swelling and shrinking were measured with a rule. In addition, the channel dimensions for efficient valve function were optimised during laser cutting by changing power and speed between 20-60% and 50-90%, respectively (in general: higher powers and lower speeds generate deeper channels). Following this, they were filled with the p(SPNIpAAm) solution and the valve gel structure photopolymerised as described above.

2.5 Ionogel-based actuator swelling and shrinking kinetics

The percentage variation in actuator height; %*H*, is defined as:

$$\%H = \frac{H_t - H_0}{H_0} \times 100 \quad (1)$$

where *H_t* is the height of the ionogel-based actuator inside the microfluidic device at time *t* and *H₀* is the height before immersion in 10⁻³ M HCl solution. The swelling kinetics were investigated by placing the ionogel-based actuator samples in 10⁻³ M HCl aqueous solution in the dark, and taking digital images every 20 min for 140 min. A single exponentially decaying growth model (Eqn.2)³² was used to calculate the swelling rate constants, following the same protocol as described by Czugala *et al.*²⁰

$$\%H = a \times (1 - e^{-k_{sw}t}) + b \quad (2)$$

where %*H* refers to the percentage of swelling, *a* is scaling factor, *k_{sw}* is the first order rate constant (s⁻¹), *b* is the baseline offset and *t* is time (s).

The shrinking kinetics of the ionogel-based actuator were investigated by irradiating with white light for 25 min. Pictures were taken with the microscope after 1, 3, 5, 10, 15 20 and 25 min of white light exposure, following the same protocol as described by us previously²⁰:

$$\%H = a \times e^{-k_{sh}t} + b \quad (3)$$

Where %*H* refers to the percentage of swelling, *a* is scaling factor, *k_{sh}* is the first order rate constant (s⁻¹), *b* is the baseline offset and *t* is time (s).

All experiments were performed at 23°C. The PMMA with the ionogel-based actuators was

positioned perpendicularly to the microscope to enable the the height of the actuators to be accurately measured. The PMMA was cut with a CO₂ laser ablation system as close as possible to the ionogel-based actuator to provide a sharp focus for precise measurements.

3 Results and Discussion

3.1 Optimisation of LoAD fabrication

In order to achieve effective fluid control, the photo-induced contraction of the ionogel must create an open channel after white light actuation. To investigate this, 1 mm diameter cylindrical reservoirs with depths between 200 μm and 500 μm were fabricated in the bottom layer of the LoAD device by applying different speed and power to the CO₂ laser, and then filling the resulting structure with the ionogel solution, Table 1, see Figure SI2. The actuator was then photopolymerised with UV light as described in the experimental section, and 3D microscope pictures were taken. After several fabrication iterations, a speed of 60% and a power of 60% were selected as the fabrication parameters for the CO₂ laser that produced an channel depth ($\sim 514 \mu\text{m}$) and actuator reservoir in the fluidic disc that gave good fluidic behaviour (i.e. effective channel opening and closing).

Table 1: Channel depths (μm) for different speeds and power (%).

Channel No.	Speed (%)	Power (%)	Channel depth (μm)
1	50	20	226.6
2	50	30	302.4
3	50	40	384.3
4	50	60	424.1
5	60	60	514.3
6	70	60	389.8
7	80	60	328.4
8	90	60	352.9

3.2 Characterisation of photo-switchable actuators swelling and shrinking kinetics

During storage, the swollen photoswitchable actuators provide effective liquid barriers as reported previously by Czugala *et al.*²⁹ Different volumes of the ionogel solution were photopolymerised *in-situ* within the microchannel. 3 μL of ionogel solution inside the reservoir area were found to produce structures that gave efficient valve behaviour. After polymerisation,

the ionogel actuators reached a height of 254 ± 46 ($n = 4$) μm after swelling for 80 min in HCl 10^{-3} M solution, exhibiting an increase of 24 % in height calculated with Eqn 1, see Figure 3A. Moreover, analysis of the height during swelling showed a linear increase occurring during the first 15 min (Figure 3A, inset). This means that during the swelling process, water diffusion is very fast until the external ionogel boundary layer in contact with the external solution is saturated/fully swollen. Thereafter, a much slower swelling process occurs from the boundary region towards the bulk, which is continuous over a much longer period of time.³³

The swollen p(SPNIpAAm) ionogel actuators are yellow due to the presence of the protonated spirobenzopyran moiety (MC-H⁺). After irradiation with white light, isomerisation to the closed-ring form (SP) was induced and the ionogel becomes colourless. This is accompanied by rapid water loss and contraction of the p(SPNIpAAm) ionogel actuator. It was found that the ionogel typically contracts by 40 ± 1 % ($n = 3$) of its initial swollen state after white light irradiation for about 5 min (Figure 3B). A stronger white light is required for shrinking of the ionogel-based actuator compared to that reported by Czugala *et al.*²² (Aigo Digital Microscope GE-5) and Benito-Lopez *et al.*³⁴ (LEDs), and despite this, the dehydration of the actuator and subsequent shrinkage is relatively slow, requiring 15 min to reach 50 ± 3 % ($n = 3$) shrinkage from its initial swollen state. However, when the material is incorporated within microfluidic devices as a valve, a smaller shrinkage percentage of $\sim 30 \pm 3$ % ($n = 3$) in 3 min is enough to open the channel (Figure 3B).

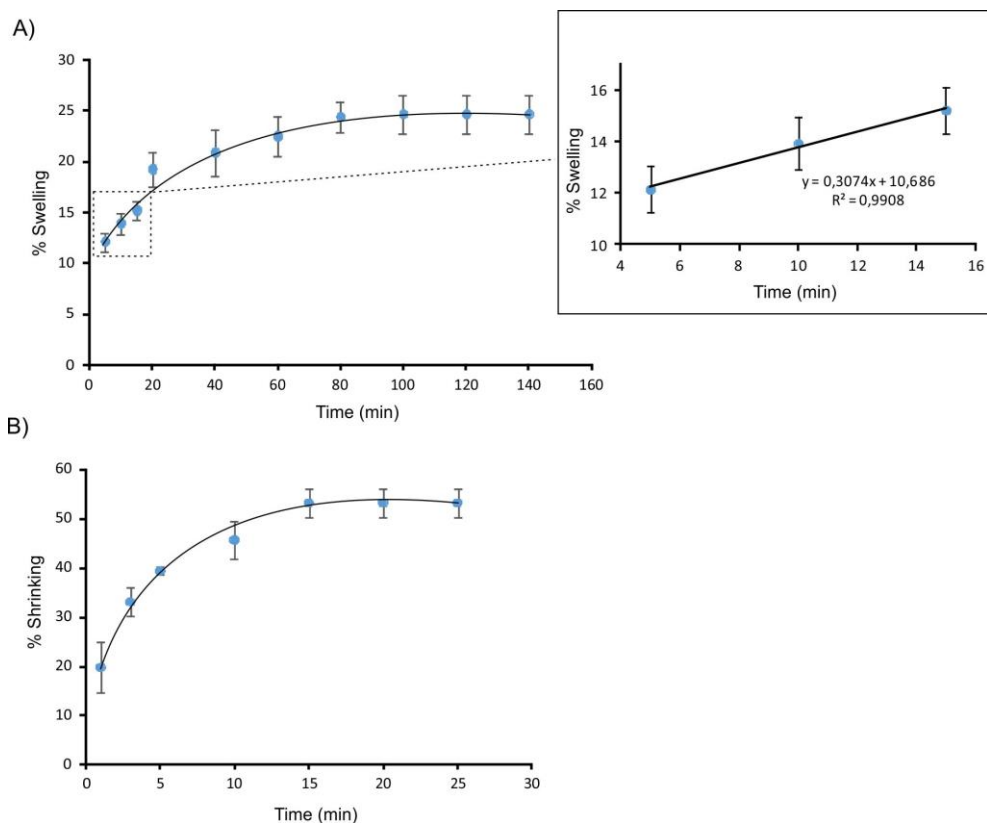


Figure 3: A) Extent of swelling as a % ($n = 4$) of the ionogel actuators inside the LoaD device versus time. A Inset) Linear trend of the %swelling vs time during the initial period (15 min) of the swelling process. B) Extent of %shrinking ($n = 3$) of the ionogel actuators inside the LoaD device versus time. The actuator behaviour was investigated in layer 4 of the LoaD device.

First-order kinetic models were fitted using Microsoft Excel Solver to the experimental data and the rate constants of the swelling process (k_{sw}) were estimated using Eqn.2. The swelling rate constant k_{sw} (black line) value obtained was $5.4 \pm 0.8 \cdot 10^{-4} \text{ s}^{-1}$ ($n = 3$). The kinetics of the shrinking behaviour of the ionogel-based actuators was followed for 25 min using white light irradiation. The rate constants of the shrinking process k_{sh} (black line) were estimated using Eqn.3 and a value of $3.5 \pm 0.6 \cdot 10^{-3} \text{ s}^{-1}$ ($n = 3$). Czugała *et al.*²² reported the swelling and shrinking kinetics of 400 μm discs made of the same p(SPNIpAAm) ionogel. Faster swelling and shrinking constants, k_{sw} of $4.5 \pm 0.3 \cdot 10^{-2} \text{ s}^{-1}$ and k_{sh} $8.3 \pm 0.9 \cdot 10^{-2} \text{ s}^{-1}$, respectively, were reported. The swelling kinetics of these gel actuators are normally dominated by diffusion-limited transport of water through the ionogel matrix, and is generally related to the energy driving the process and to the surface area to volume ratio (SA/V).²² Therefore, smaller ionogels should improve the swelling process since the rate of diffusion is inversely proportional to the first power dimension of the ionogel. The swelling behaviour of the ionogel in the LoaD device is, as demonstrated by others before,³³ determined by the balance between the expanding force induced by the osmotic pressure of

polymer solvation and the restoring force of the chain segments between crosslinks. Moreover, the PMMA reservoir restricts the movement of the actuator, and therefore the swelling occurs anisotropically from the bottom surface of the LoAD towards the main channel in the z -axis direction. In the LoAD platform the ionogels dimensions are bigger, 1 mm versus 0.4 mm from Czugala's findings, and the surface area to volume ratio are smaller, due to the ionogel constriction inside the microfluidic reservoir, and therefore it is not surprising that the actuation kinetics are slower for the LoAD valves.

Figure 4A shows the volume phase transition of the actuators induced by water intake and subsequent white light irradiation over time. It can be clearly observed that the ionogel actuators expanded enough to block the main channel and contracted enough under white light irradiation to open it. Figure 4B shows 3D microscope pictures of the same dehydrated, expanded and contracted actuator represented in Figure 4A. In the initial dehydrated state, the maximum height of the ionogel actuator and the PMMA sheet are the same $\sim 230 \mu\text{m}$, when hydrated the observed maximum height is $\sim 266 \mu\text{m}$ (channel closed), decreasing to $\sim 190 \mu\text{m}$ when contracted (channel open).

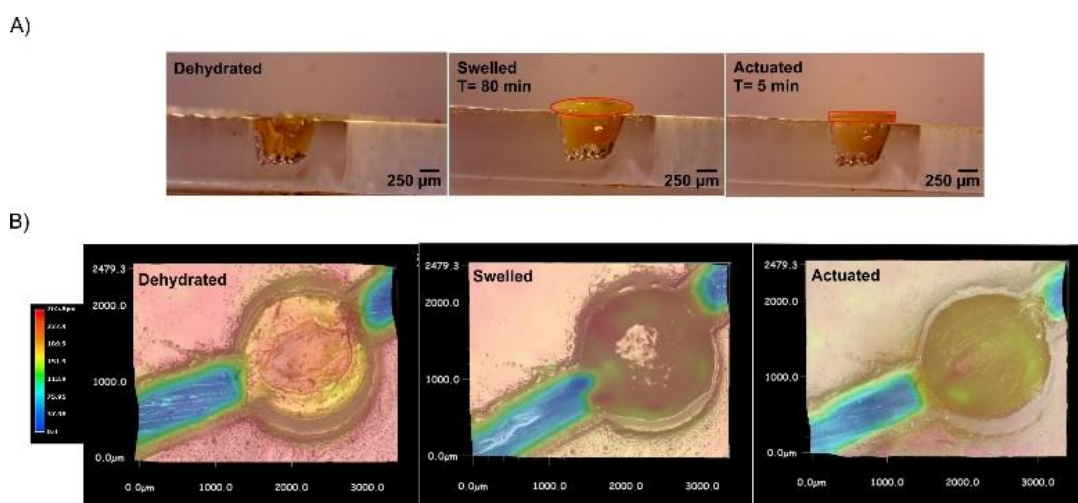


Figure 4: A) Set of pictures showing the initial dehydrated (left), hydrated (centre, closed) and contracted (right, open) states of the ionogel actuator inside the LoAD device (a red highlight has been added to the pictures to show the degree of swelling and shrinking of the ionogel). B) Set of 3D microscope pictures showing the initial dehydrated state followed by the hydrated (closed) and contracted (open) states with colour-matched heights of the ionogel actuator inside the LoAD device over time.

3.2 Regeneration of the ionogel actuator inside the LoAD device

The p(SPNIPAAm) ionogel based actuators require exposure to an acidic solution (pH = 3) to induce swelling, whereas the shrinking mechanism results in the release of protons and water into external solution from the ionogel.¹⁴ The actuator is first soaked in an aqueous solution of HCl 10⁻³ M in order to induce isomerisation to the protonated merocyanine (MC-H⁺) form. Then the ionogel swells and adopts a more hydrophilic conformation to the extent that the actuator blocks the main channel. After irradiation with white light, the MC-H⁺ isomer reverts to the uncharged, colourless SP form, which triggers dehydration and shrinkage of the actuators, unblocking of the main channel in the process.²⁰ In order to evaluate the reusability of the actuator and thus its regeneration in the LoAD device, several cycles of re-swelling of the actuator with HCl solution and subsequent actuation with white light were carried out, Figure 5. It was found that the actuator function was maintained for up to 3 cycles of regeneration/actuation after which degradation of the ionogel actuator was observed, see cycle 4 in Figure 5. In order to evaluate the percentage deviation of the performance of the actuator after several regeneration/actuation cycles, the hysteresis of the ionogel-based actuator in cycles 2, 3 and 4 was calculated. It was found that, after cycle 3, a hysteresis of 80% for regeneration (swelling) and 77% for photo-induced contraction occurred, which was insufficient for fluidic control (valve failure). A smaller degree of hysteresis was found for cycles from 1 to 3 (30 % higher). *Delaney et al.*³⁵ recently suggested that the first few cycles could be anomalous, due to settling of the system, as this appears to be followed by a longer period of reproducibility over multiple cycles. In our case, the hysteresis caused failure because the ionogel was too swollen, leading to permanent channel blockage. This effect can be reduced by creating the ionogel microactuator structure using photopolymerisation through a mask instead of actual drop casting protocol used in this study.³⁵

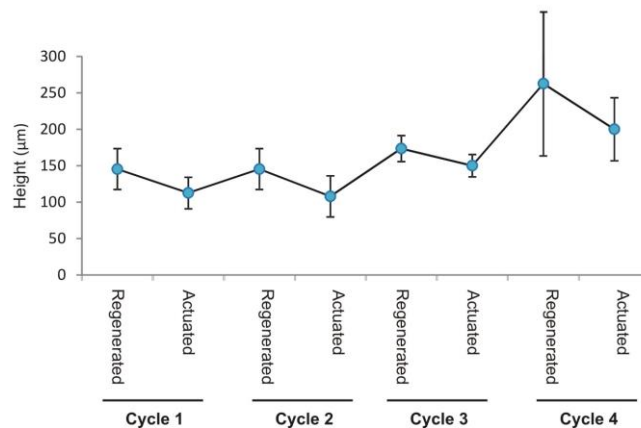


Figure 5: Regeneration cycles using HCl 10⁻³ M (pH = 3) solution followed by actuation with white

light of the ionogel actuators ($n = 3$).

3.3 Performance of the LoaD valve actuator

The performance of the ionogel-based valve actuator in the LoaD device was investigated. The microfluidic structure consisted of two chambers connected by a channel in which the ionogel-based actuator was placed. Another perpendicular channel passed to the actuator, from the reverse side of the main fluidic channel, to provide a source of acid to the ionogel for re-swelling of the valve actuator after contraction under white light irradiation, Figure 6. The upper chamber was filled with a coloured dye solution for visualisation of the process (Figure 6A). Disc rotation at 600 rpm moved the coloured solution towards the bottom of the chamber. The actuator at this stage blocks the main channel, preventing the sample from moving along the channel that connects both chambers. After this, white light irradiation was applied for 3 min in order to contract the ionogel valve and open the channel. The fluid now moves to the bottom chamber, emptying the upper chamber (Fig. 6B). This mechanism can be repeated at least three times due to the perpendicular channel which exposes the ionogel actuator to the acidic solution, by rotating the disc at 400 rpm, (Figure 6, C and D). This solution induces the re-swelling of the actuators after about 20 min to the extent that the channel is once more closed.

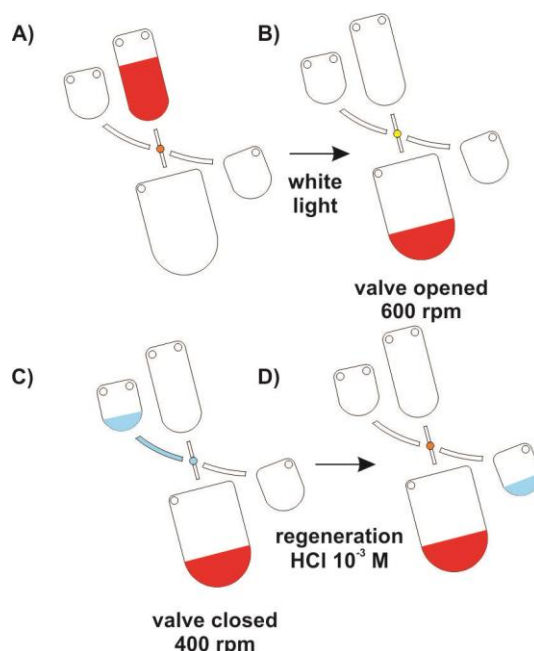


Figure 6: Schematic of actuator valve operation in the LoaD device. A) 40 μL of red dye is loaded. The disc is rotated at 600 rpm and the red dye solution moves to bottom side of the upper chamber but cannot pass further due to the swollen (closed) valve (red dot in the channel). B)

The ionogel-based actuator is exposed to white light for 3 min. The actuator opens (yellow dot) and the red dye solution passes from the upper to the lower chamber through the now open connecting channel. C) Spinning is stopped and 40 μL of $\text{HCl } 10^{-3} \text{ M}$ (blue) is loaded in the upper regeneration chamber. The LoaD is rotated at 400 rpm and the blue acidic solution passes from the upper to the lower regeneration chamber, causing re-swelling of the gel actuator (blue dot, 20 min for total re-swelling of the ionogel). The gel valve is then ready for a repeat cycle (red dot). Note that at all times, the gel prevents transfer of the acid from the regeneration chambers into the main channel and chambers.

Figure 7 presents a set of pictures taken from the video, Video-1, which show the performance of the ionogel actuator in the LoaD. The actuator was covered with an opaque tape to protect it from ambient light during device storage.

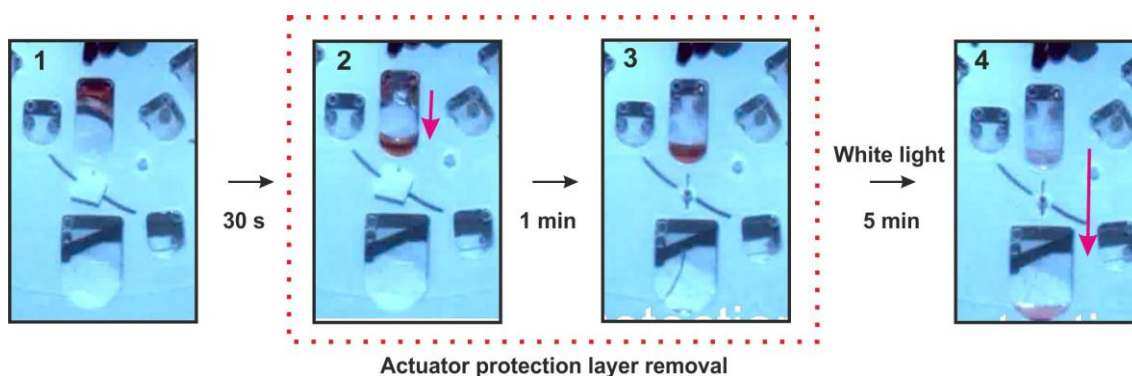


Figure 7: Set of pictures taken from a video (high speed camera) during actuator performance at 600 rpm. 1) The coloured dye solution is loaded in the upper chamber and the actuator is shielded from light with a PSA layer. 2) The disc spins at 600 rpm and the sample moves to the bottom part of the upper chamber due to centrifugal forces. 3) The PSA layer is removed and 4) upon white light irradiation, the actuator shrinks and the sample passes from the upper to the lower chamber.

This design and position of the perpendicular channel and chambers ensures that no acid solution accesses the main channel during the actuator regeneration-spinning step as the ionogel-based actuator acts as a physical barrier between the regeneration channel and the main channel at all times. However, the design of the regeneration channel ensures effective exposure to acidic solution when required, leading to the re-swelling of the actuator, which can be initiated by applying a disc rotation speed of 400 rpm.

Finally, the burst threshold of the actuator was found to be between 750-800 rpm. Therefore

speeds below these values are able to provide a stable physical barrier for the LoAD device. Stronger sealing can be achieved by changing the chemistry of the ionogel using more hydrophobic ionic liquids and/or higher cross-linked gels. However, this will also affect the actuation response and swelling/shrinking kinetics of the gel, which needs to be considered during the fabrication of the LoAD device.

4 Conclusions

We have demonstrated that a reusable ionogel-based photoactuator can be operated successfully within a microfluidic channel without complex actuator designs or reverting to single use dissolvable/wax actuators. It was found out that the p(SPNIpAAm) ionogel-based actuator swelling and contraction rate constants inside the microfluidic device were $5.4 \pm 0.8 \cdot 10^{-4} \text{ s}^{-1}$ and $3.5 \pm 0.6 \cdot 10^{-3} \text{ s}^{-1}$, respectively. It has been shown that the ionogel-based actuator provides a reasonably well-defined degree of volume change (%*H*) and photoresponse time inside the microfluidic device. This could have important implications for the practical implementation of disc-based microfluidics, as it potentially opens the way towards the generation of lab on a disc microfluidic systems in which the photonic actuation stimulus can be totally separated from the reagents, which is compatible with a freely spinning disc configuration. It also opens the possibility of multiple use valves, by re-swelling the p(SPNIpAAm) ionogel with an acidic solution in a perpendicular channel.

5 Acknowledgements

FBL acknowledges the Ramón y Cajal Programme (Ministerio de Economía y Competitividad), Spain. This project has received funding from the European Union's Seventh Framework Programme (FP7) for Research, Technological Development and Demonstration under grant agreement no. 604241. JS and FBL acknowledge funding support from Gobierno de España, Ministerio de Economía y Competitividad, with Grant No. BIOMINECO –P and personally acknowledge to Marian M. De Pancorbo for letting them to use her laboratory facilities at UPV/EHU. A.T., L.F., and D.D. are grateful for financial support from the Marie Curie Innovative Training Network OrgBIO (Marie Curie ITN, GA607896) and Science Foundation Ireland (SFI) under the Insight Centre for Data Analytics initiative, Grant Number SFI/12/RC/2289.

6 References

- 1 O. Strohmeier, M. Keller, F. Schwemmer, S. Zehnle, D. Mark, F. Von Stetten, R. Zengerle and N. Paust, *Chem. Soc. Rev.*, 2015, **44**, 6187-6229.
- 2 M. Tang, G. Wang, S. Kong and H. Ho, *Micromach.*, 2016, **7**,1-29.
- 3 T. Kim, V. Sunkara, J. Park, C. Kim, H. Woo and Y. Cho, *Lab Chip*, 2016, **16**, 3741-3749.
- 4 J. Xiang, Z. Cai, Y. Zhang and W. Wang, *Sens. Actuators B, Chem*, 2017, **243**, 542-548.
- 5 R. Gorkin, C. E. Nwankire, J. Gaughran, X. Zhang, G. G. Donohoe, M. Rook, R. O'Kennedy and J. Ducreé, *Lab Chip*, 2012, **12**, 2894-2902.
- 6 Z. Cai, J. Xiang, H. Chen and W. Wang, *Sens. Actuators B, Chem*, 2016, **228**, 251-258.
- 7 S. Zehnle, F. Schwemmer, R. Bergmann, F. von Stetten, R. Zengerle and N. Paust, *Microfluid. Nanofluid.*, 2015, **19**, 1259-1269.
- 8 O. Ymbern, P. Couceiro, M. Berenguel-Alonso, N. Sáñez and J. Alonso, *Int. Conf. Miniaturized Syst. Chem. Life Sci., MicroTAS*, 2016, 1055-1056.
- 9 M. Keller, A. Drzyzga, F. Schwemmer, R. Zengerle and F. Von Stetten, *Int. Conf. Miniaturized Syst. Chem. Life Sci., MicroTAS*, 2015, 1184-1186.
- 10 L. X. Kong, K. Parate, K. Abi-Samra and M. Madou, *Microfluid. Nanofluid.*, 2015, **18**, 1031-1037.
- 11 D. J. Kinahan, S. M. Kearney, N. Dimov, M. T. Glynn and J. Ducreé, *Lab Chip*, 2014, **14**, 2249-2258.
- 12 D. J. Kinahan, S. M. Kearney, O. P. Faneuil, M. T. Glynn, N. Dimov and J. Ducreé, *RSC Adv.*, 2015, **5**, 1818-1826.
- 13 C. E. Nwankire, M. Czugala, R. Burger, K. J. Fraser, T. M. Connell, T. Glennon, B. E. Onwuliri, I. E. Nduaguibe, D. Diamond and J. Ducreé, *Biosens. Bioelectron.*, 2014, **56**, 352-358.
- 14 R. Klajn, *Chem. Soc. Rev.*, 2014, **43**, 148-184.
- 15 Y. Maeda, T. Higuchi and I. Ikeda, *Langmuir*, 2001, **17**, 7535-7539.
- 16 H. G. Schild, *Prog Polym Sci (Oxford)*, 1992, **17**, 163-249.
- 17 C. Boutris, E. G. Chatzi and C. Kiparissides, *Polym.*, 1997, **38**, 2567-2570.
- 18 X. Zhang, Y. Yang, T. Chung and K. Ma, *Langmuir*, 2001, **17**, 6094-6099.
- 19 S. Sugiura, K. Sumaru, K. Ohi, K. Hiroki, T. Takagi and T. Kanamori, *Sens. Actuators A, Phys*, 2007, **140**, 176-184.

- 20 L. Florea, D. Diamond and F. Benito-Lopez, *Macromol. Mater. Engin.*, 2012, **297**, 1148-1159.
- 21 S. Gallagher, L. Florea, K. J. Fraser and D. Diamond, *Int. J. Mol. Sci.*, 2014, **15**, 5337-5349.
- 22 M. Czugala, C. O'Connell, C. Blin, P. Fischer, K. J. Fraser, F. Benito-Lopez and D. Diamond, *Sens. Actuators B, Chem*, 2014, **194**, 105-113.
- 23 A. Akyazi, J. Saez, A. Tudor, C. Delaney, W. Francis, D. Diamond, L. Basabe-Desmonts, L. Florea and F. Benito-Lopez, in *in Ionic liquid devices*, ed. ed. A. Eftekhari, Royal Society of Chemistry, 2018.
- 24 F. Benito-Lopez, M. Antoñana-Díez, V. F. Curto, D. Diamond and V. Castro-López, *Lab Chip*, 2014, **14**, 3530-3538.
- 25 B. Ziólkowski, L. Florea, J. Theobald, F. Benito-Lopez and D. Diamond, *Soft Mat.*, 2013, **9**, 8754-8760.
- 26 S. Coleman, J. ter Schiphorst, A. Azouz, S. Ben Bakker, A. P. H. J. Schenning and D. Diamond, *Sens. Actuators B, Chem*, 2017, **245**, 81-86.
- 27 M. Czugala, D. Maher, F. Collins, R. Burger, F. Hopfgartner, Y. Yang, J. Zhaou, J. Ducreé, A. Smeaton, K. J. Fraser, F. Benito-Lopez and D. Diamond, *RSC Adv.*, 2013, **3**, 15928-15938.
- 28 A. Szilágyi, K. Sumaru, S. Sugiura, T. Takagi, T. Shinbo, M. Zrínyi and T. Kanamori, *Chem. Mater.*, 2007, **19**, 2730-2732.
- 29 M. Czugala, C. Fay, N. E. O'Connor, B. Corcoran, F. Benito-Lopez and D. Diamond, *Talanta*, 2013, **116**, 997-1004.
- 30 T. Glennon, J. Saez, M. Czugala, L. Florea, E. McNamara, K. J. Fraser, J. Ducree, D. Diamond and F. Benito-Lopez, *2015 Transducers - 2015 18th International Conference on Solid-State Sensors, Actuators and Microsystems, TRANSDUCERS 2015*, 2015, 109-112.
- 31 J. Saez, L. Basabe-Desmonts and F. Benito-Lopez, *Microfluid. Nanofluid.*, 2016, **20**:116.
- 32 D. Diamond and V. C. A. Hanratty, *Spreadsheet applications in chemistry using microsoft excel*, Wiley, Dublin, 1997.
- 33 A. Mateescu, Y. Wang, J. Dostalek and U. Jonas, *Membranes*, 2012, **2**, 49-69.
- 34 F. Benito-Lopez, R. Byrne, A. M. Radut^a, N. E. Vrana, G. McGuinness and D. Diamond, *Lab Chip*, 2010, **10**, 195-201.
- 35 C. Delaney, P. McCluskey, S. Coleman, J. Whyte, N. Kent and D. Diamond, *Lab Chip*, 2013, **17**, 2013-2021.